

Title: A high-throughput, automated, cell-free expression and screening platform for antibody discovery

Authors: Andrew C. Hunt^{1,2}, Bastian Vögeli^{1,2}, Weston K. Kightlinger^{1,2}, Danielle J. Yoesep^{1,2}, Antje Krüger^{1,2}, Michael C. Jewett^{1,2,3,4*}

Affiliations:

¹Department of Chemical and Biological Engineering, Northwestern University, Evanston, IL, 60208, USA

²Center for Synthetic Biology, Northwestern University, Evanston, IL, 60208, USA

³Chemistry of Life Processes Institute, Northwestern University, Evanston, IL, 60208, USA

⁴Robert H. Lurie Comprehensive Cancer Center, Northwestern University, Chicago, IL, 60611, USA

*Corresponding author: Michael Jewett (m-jewett@northwestern.edu)

Abstract

Antibody discovery is bottlenecked by the individual expression and evaluation of antigen-specific hits. Here, we address this gap by developing an automated workflow combining cell-free DNA template generation, protein synthesis, and high-throughput binding measurements of antibody fragments in a process that takes hours rather than weeks. We apply this workflow to 119 published SARS-CoV-2 neutralizing antibodies and demonstrate rapid identification of the most potent antibody candidates.

Main Body

Antibodies are widely used as protein-based drugs and diagnostics. They are the critical component in immunoassays enabling rapid diagnostics¹ and constitute one of the fastest-growing classes of therapeutics with nearly 25% of new FDA-approved drugs in 2020 being antibodies^{2,3}. Antibodies have also recently garnered attention as potential countermeasures for emerging pathogens, and currently constitute the majority of emergency use authorized treatments for COVID-19 that inhibit the SARS-CoV-2 virus⁴⁻⁶.

Modern workflows for antibody discovery utilize either directed evolution or the isolation of single B-cell clones from convalescent patients or animals to go from $>10^8$ possible sequences to a pool of $\sim 10^3$ candidates targeting the desired antigen. However, once this pool of candidates has been generated, state-of-the-art workflows still rely on labor-intensive and poorly scalable procedures (e.g., plasmid-based cloning, transfection, cell-based protein expression, protein purification, binding assessment through enzyme-linked immunosorbent assays (ELISAs), etc.) to individually evaluate and identify the best antibody candidates^{7,8}. These labor-intensive procedures take weeks to months and represent a major bottleneck in antibody discovery. The effort to identify antibodies against emerging threats like the SARS-CoV-2 during the COVID-19 pandemic has highlighted (i) the importance of rapid and high-throughput antibody discovery platforms and (ii) the importance of identifying high-affinity antibodies targeting conserved epitopes^{9,10} or non-overlapping epitopes^{11,12} to resist viral escape and increase the ability to neutralize viral variants^{13,14}; both of which have required intensive screening campaigns. A further challenge is that existing antibody discovery processes frequently have low efficiency, with very few of the screened candidates being potent neutralizers in the case of SARS-CoV-2 (Supplementary Table 1). Taken together, these limitations in existing antibody discovery processes suggest the urgent need for faster and higher throughput screens.

Cell-free protein synthesis (CFPS)^{15,16}, the manufacture of proteins without living cells using crude extracts or purified components, is an attractive tool to overcome these limitations. Towards this goal, a variety of CFPS systems for antibody expression have been developed¹⁷⁻²³. However, to our knowledge, an end-to-end (DNA to data) automatable antibody screening workflow combining CFPS with a high-throughput protein-protein interaction screen has yet to be developed.

Here we describe such an integrated pipeline for antibody expression and evaluation to address critical screening limitations in current antibody discovery pipelines. The workflow leverages four key developments (Fig. 1a): (i) DNA assembly and amplification methods that do not require living cells, (ii) CFPS systems that can work directly from linear DNA templates and can generate disulfide-bonded antibody molecules, (iii) an Amplified Luminescent Proximity Homogeneous Linked Immunosorbent Assay (AlphaLISA) that enables rapid protein-protein interaction (PPI) or binding characterization without protein purification²⁴, and (iv) robotic and acoustic liquid handling that enables a highly parallel and miniaturized workflow. Our integrated workflow is end-to-end automatable and enables a single researcher to express and profile the antigen-specific binding of hundreds of antibodies in 24 hours. As a model, we applied our workflow to profile a diverse set of 120 previously published antibodies, 119 of which are antibodies targeting the SARS-CoV-2 spike glycoprotein (S trimer). These antibodies were selected based on the availability of sequence, structural, SARS-CoV-2 neutralization, and binding information, with 84 being drawn from Brouwer *et al.*²⁵ and the remainder from diverse sources^{9,26–40} (Supplementary Table 2 and 3). The antibodies span four orders of magnitude in neutralization potency and target a variety of domains and epitopes.

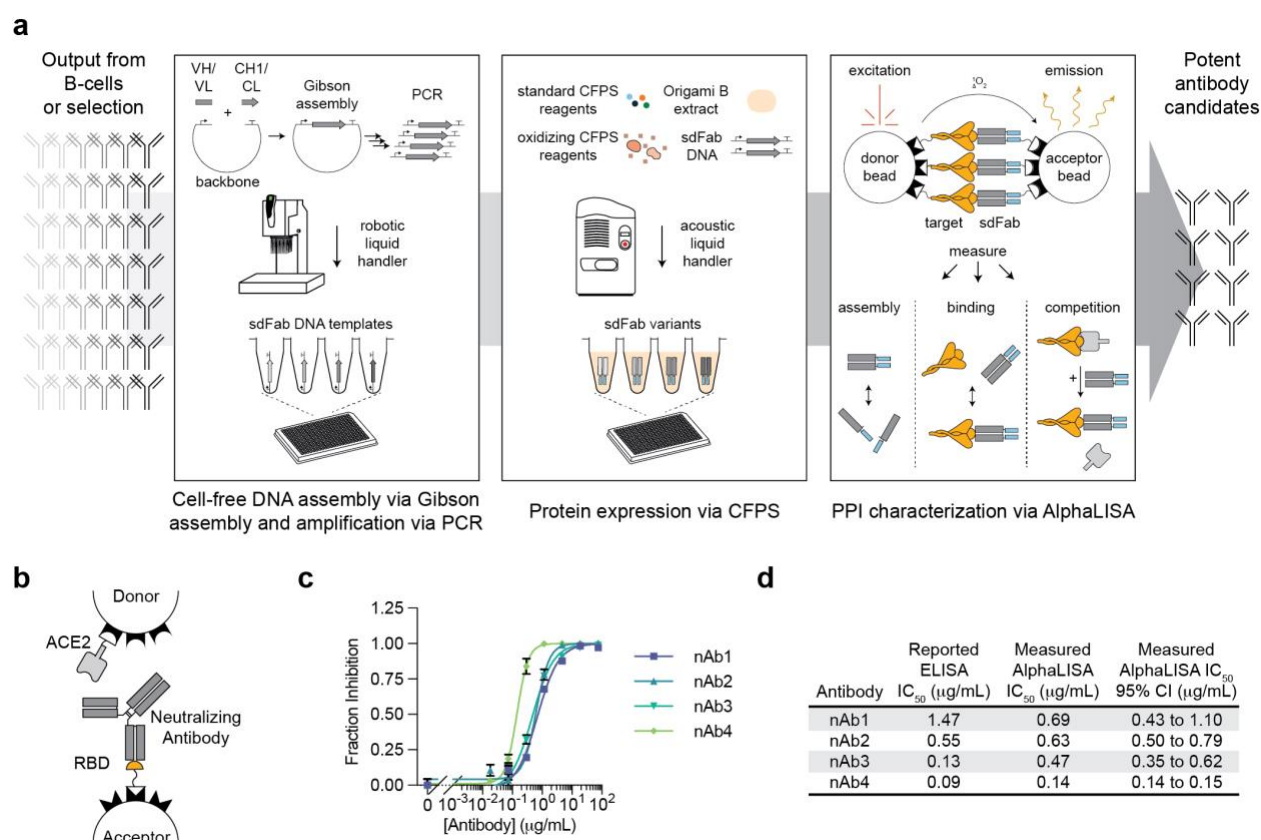


Fig. 1 | A high-throughput, cell-free antibody screening workflow. a, Schematic of the steps involved in the cell-free antibody screening workflow. **b**, Diagram of the AlphaLISA screen for neutralizing antibodies via competition with ACE2 for the SARS-CoV-2 RBD. **c**, Evaluation of commercial neutralizing antibodies (nAbs) in the AlphaLISA ACE2 competition screen (n=3 independent replicates ± SEM). **d**, Comparison of the reported and measured potencies of commercial neutralizing antibodies.

We first implemented a cell-free method for DNA assembly and amplification by adapting and optimizing recently reported protocols for high-throughput construction of DNA templates for CFPS^{17,19,41,42}. The method consists of a Gibson assembly step, followed by PCR amplification of the linear expression template (LET) using the unpurified Gibson assembly product as a template. The key idea was to create a versatile approach for rapid construction of DNA templates without the requirement of cell culture, allowing DNA assembly and amplification in less than 3 hours entirely in 384 well plates. To validate the method, we applied it to the assembly and amplification of a LET for sfGFP expression and only observed sfGFP expression in the presence of properly assembled DNA template (Supplementary Fig. 1a-c). To assemble antibody DNA templates, we purchased synthetic, double-stranded linear DNA coding for the desired variable heavy (VH) and variable light (VL) chain sequences. These DNAs were assembled with DNA coding for the appropriate heavy chain constant (CH1) or light chain constant (CL) antigen-binding fragment (Fab) domains in addition to a separate piece of DNA coding for the backbone of the pJL1 vector. These sequences were subsequently amplified by PCR to generate LETs (Supplementary Fig. 1d-f). Previous works suggest that this workflow could be compatible with PCR products amplified from single B-cells from an immunized animal^{17,19,41}. In addition to being fast, this workflow also affords flexibility, allowing assembly of different antibody formats (e.g., full-length, Fab, sdFab) containing different purification or immobilization tags by using different antibody constant regions in the assembly reaction.

We next demonstrated rapid antibody expression in a crude *E. coli* based CFPS system. We developed a high-yielding ($1,390 \pm 32$ $\mu\text{g/mL}$ sfGFP, Supplementary Fig. 1c) crude *E. coli* lysate-based CFPS system from the OrigamiTM B(DE3) strain (Supplementary Fig. 2), which contains mutations in the *E. coli* reductase genes *trxB* and *gor* to enable the formation of disulfide bonds in the cytoplasm⁴³. By pretreating the extract with the reductase-inhibitor iodoacetamide (IAM) to further stabilize the redox environment^{44–46} and supplementing the reaction with purified *E. coli* disulfide bond isomerase DsbC and prolyl isomerase FkpA^{20,47,48}, we successfully expressed and assembled full-length trastuzumab, a model anti-HER2 antibody⁴⁹, from linear DNA templates (Supplementary Fig. 2a). However, like others^{17–21}, we found that the efficient assembly of full-length antibodies in CFPS can require further optimization (e.g., temperature, DNA template ratio, DNA template expression timing) which is not optimal for high-throughput screening. Like reports by Ojima-Kato *et al.*^{17–19}, we found that the assembly of synthetically dimerized antigen-binding fragments (sdFab, also called ecobodies^{17,19} or zipbodies¹⁸) were more consistent than their corresponding standard Fabs in CFPS for a small panel of antibodies and opted to utilize the sdFab format for expression (Supplementary Fig 2b-c). Using acoustic liquid handling we can assemble CFPS reactions to express each sdFab variant from cell-free assembled and amplified DNA in 384-well plates (Fig. 1a).

Following DNA assembly and CFPS, antigen-specific binding was evaluated. To characterize the PPIs of the expressed sdFab antibody candidates, we developed an AlphaLISA method to characterize PPIs directly from CFPS reactions. AlphaLISA is an in-solution and wash-free assay that is designed for high-throughput screening and is

compatible with crude cell-lysates²⁴. In AlphaLISA, non-covalent capture chemistries are used to immobilize the proteins of interest on donor and acceptor beads, which generate a chemiluminescent signal when in proximity of one another and excited by a 680 nm laser. We developed AlphaLISA methods to enable the measurement of both direct binding to an antigen as well as competition for specific epitopes. We first sought to validate that AlphaLISA is tolerant of crude CFPS reactions. We observed that CFPS does not interfere with the measurement chemistry (Supplementary Fig. 3a), but that certain reaction components can disrupt protein immobilization to the bead which can be circumvented with the appropriate choice of immobilization chemistry (Supplementary Fig 3b-c). We found that the Ni-Chelate beads were not tolerant of the high salt concentrations and high concentration of histidine present in CFPS, likely due to charge screening and Ni chelation respectively hindering immobilization of the hisx6 tagged protein. To validate the ability of AlphaLISA to profile neutralizing antibodies, we tested the ability of five different commercial antibodies to compete with the SARS-CoV-2 target human receptor Angiotensin-Converting Enzyme 2 (ACE2) for binding of the SARS-CoV-2 Receptor Binding Domain (RBD) and found that our determined rank order of IC₅₀ values aligns with the reported ELISA IC₅₀'s (Fig. 1b-d). Further, we utilized AlphaLISA to develop a sdFab assembly screen to monitor antibody expression and assembly in CFPS, a laborious step that traditionally requires SDS-PAGE. The measurement immobilizes the heavy and light chains of the sdFab to the AlphaLISA beads, resulting in signal when the two chains are assembled (Supplementary Fig. 3d). The AlphaLISA assembly assay shows consistent prediction of antibody assembly with SDS-PAGE on a panel of sdFabs and can thus be used to identify when sdFab expression or assembly fails (Supplementary Fig. 3e).

Using the developed workflow, we next evaluated a set of 120 unique antibodies using AlphaLISA to measure antibody binding to the SARS-CoV-2 S trimer, binding to the SARS-CoV-2 RBD, competition with ACE2 for RBD binding, and assembly of their heavy and light chains in CFPS (Fig. 1a and Fig. 2). Antibodies were expressed and evaluated in triplicate. AlphaLISA replicates were found to be consistent with one another, validating that the acoustic liquid handling workflow is robust (Supplementary Fig. 4). Samples were evaluated for significant assembly, binding to, or competition with a given target using a two-sided student's t-test corrected for multiple testing using the Benjamini and Hochberg False Discovery Rate procedure (FDR)⁵⁰. Within the diverse set of 36 antibodies, we observed assembly for 36 out of 36 tested antibodies, S trimer binding for 28 out of 35 antibodies reported to bind the S trimer, RBD binding for 23 out of the 34 antibodies reported to bind the RBD, and ACE2 competition for 16 out of 31 antibodies reported to compete with ACE2 (Fig. 2a, Supplementary Fig. 5). For the set of 84 antibodies from Brouwer *et al.*, we observed assembly of 80 out 84 antibodies and binding to the S trimer and RBD for many of the antibodies that showed strong binding via ELISA (Fig. 2b-d). We compared ACE2 competition against neutralization since it has been reported that more than 90% of neutralizing antibodies block the RBD and ACE2 interaction^{28,51} and similar competition assays have been reported to correlate with neutralization potency^{28,52} (Fig. 2e). We observed ACE2 competition, as well as strong S trimer and RBD binding, for 4 out of 5 antibodies reported to compete with ACE2, which also represent the four most potent neutralizers in the Brouwer *et al.* data set.

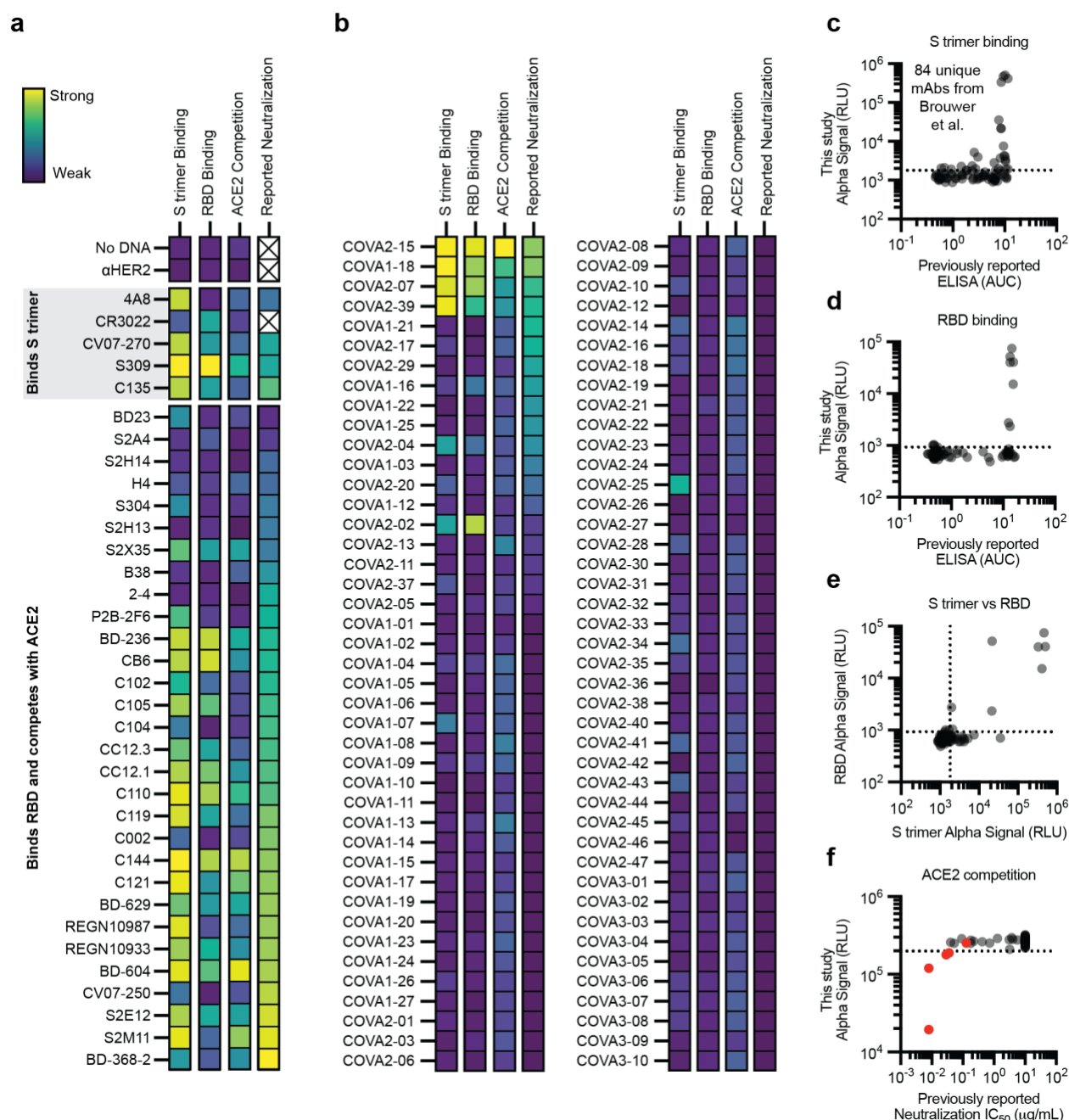


Fig. 2 | Performance of the cell-free antibody screening workflow evaluated on SARS-CoV-2 neutralizing antibodies. a-f, AlphaLISA data are presented as the mean of 3 independent replicates. A dashed line indicates three standard deviations away from the background signal. **a-b**, Heatmap of the binding of previously published antibodies measured using AlphaLISA to detect S trimer binding (log₁₀ scaled), RBD binding (log₁₀ scaled), and ACE2 competition (linearly scaled). AlphaLISA data are presented as the mean of 3 independent replicates. The lowest reported neutralization IC₅₀ value is also plotted for comparison (log₁₀ scaled) and an X indicates no relevant data available (Supplementary Table 2). **a** Heatmap of the binding of 36 diverse antibodies. **b**, Heatmap of the binding of all 84 antibodies in the Brouwer *et al.* data set. **c-d**, Parity plots comparing the AlphaLISA the 84 antibodies in the Brouwer *et al.* data set vs the published ELISA data. A dashed line indicates three standard deviations away from the background. **c**, S trimer binding. **d**, RBD binding. **e**, Comparison of the S trimer and RBD AlphaLISA binding

data. **f**, Parity plot comparing the AlphaLISA ACE2 competition data for the 84 antibodies in the Brouwer *et al.* data set vs the published pseudovirus neutralization data. Antibodies that were reported to compete with ACE2 by Brouwer *et al.* are plotted in red.

Notably, we observed ACE2 competition for 10 out of 13 antibodies in the overall data set whose neutralization IC₅₀ values are less than 0.01 µg/mL. While some less-effective neutralizers could not be completely characterized in our screen, we consistently identified potent neutralizing antibodies in our rapid cell-free screening workflow whose mechanism is ACE2 competition. Consistent with their binding specificities, we observed that 4A8, an n-terminal domain targeted antibody³⁷, only showed strong interaction with the S trimer and that CR3022, whose target epitope is occluded in the S trimer^{34,53}, showed binding to the RBD, but weak binding to the S trimer. Surprisingly, the S309 antibody in the sdFab format exhibited competition with ACE2 although it has been previously reported not to compete with ACE2⁹, which will require further study. Taken together, the binding and competitive AlphaLISA data generated by our workflow are self-consistent and largely align with the literature (Supplementary Table 4). Further improvements to the dynamic range of the PPI measurements could broaden the utility for performing antigenic mapping of the immune response to antigens. Inclusion of other binding targets could allow researchers to easily evaluate targeting to different domains (e.g., SARS-CoV-2 N-terminal domain) or look for antibodies targeting conserved epitopes by evaluating cross-reactivity with other related viruses (e.g., SARS-CoV, etc.).

In summary, we developed an integrated and automated workflow for antibody screening by combining methods for cell-free DNA assembly and amplification, cell-free protein expression, and highly parallel binding characterization via AlphaLISA. This workflow has two key features. First, it is fast. The entire workflow for all 120 antibodies evaluated in this study was completed in triplicate in less than 24 hours in two consecutive working days by a single researcher, highlighting the workflow's speed and throughput. Second, integration of the AlphaLISA assay in cell-free extracts without the need for protein purification facilitates direct evaluation of synthesized antibodies in high-throughput. This is important because this is frequently the limiting step in previously published methods. Looking forward, we anticipate that the increased speed and throughput afforded by our workflow will enable researchers to easily and rapidly screen thousands of antibodies, facilitating down-selection to a few highly potent candidates that can be expressed at larger scales in cells or using CFPS and subjected to deeper developability testing. In this way, our method is poised to aid in the discovery of medical countermeasures in future pandemics, and more broadly, in the development of antibodies for therapeutic, diagnostic, and research applications.

Acknowledgments

We thank Ashty S. Karim (ORCID 0000-0002-5789-7715) for discussions about research direction and comments on the manuscript and Kosuke Seki for the donation of the fLuc plasmid. M.C.J. acknowledges support from the David and Lucile Packard Foundation, the Camille Dreyfus Teacher-Scholar Program, and the Defense Threat Reduction Agency Grants HDTRA1-15-10052, HDTRA-12-01-0004, and HDTRA-12-11-0038. A.C.H. was supported by a Department of Defense National Defense Science and Engineering Graduate (NDSEG) Fellowship (NDSEG-36373).

Author Contributions

A.C.H., B.V., and M.C.J. conceived of the study. A.C.H., B.V., and A.K.G. completed the research. W.K.K. and D.J.Y. assisted with cell-free expression methods. M.C.J. supervised the research. A.C.H. wrote the manuscript. All authors commented on and edited the manuscript.

Competing Interests

A.C.H. has consulted for SwiftScale Biologics. W.K.K. and D.J.Y. are current employees of SwiftScale Biologics. M.C.J. is a cofounder of SwiftScale Biologics, Stemloop, Inc., Design Pharmaceuticals, and Pearl Bio. M.C.J.'s interests are reviewed and managed by Northwestern University in accordance with their conflict-of-interest policies. All other authors declare no competing interests.

References

1. Koczula, K. M. & Gallotta, A. Lateral flow assays. *Essays in Biochemistry* **60**, 111–120 (2016).
2. Lu, R.-M. *et al.* Development of therapeutic antibodies for the treatment of diseases. *Journal of Biomedical Science* **27**, 1 (2020).
3. Mullard, A. 2020 FDA drug approvals. *Nature Reviews Drug Discovery* **20**, 85–90 (2021).
4. FDA. Emergency Use Authorization for REGEN-COV (Casirivimab and Imdevimab). <https://www.fda.gov/media/145610/download> (2020).
5. FDA. Emergency Use Authorization for Bamlanivimab and Etesevimab. <https://www.fda.gov/media/145801/download> (2020).
6. FDA. Emergency Use Authorization for Sotrovimab. (2021).
7. Vazquez-Lombardi, R. *et al.* Transient expression of human antibodies in mammalian cells. *Nature Protocols* **13**, 99–117 (2018).
8. Gieselmann, L. *et al.* Effective high-throughput isolation of fully human antibodies targeting infectious pathogens. *Nature Protocols* **16**, 3639–3671 (2021).
9. Pinto, D. *et al.* Cross-neutralization of SARS-CoV-2 by a human monoclonal SARS-CoV antibody. *Nature* **583**, 290–295 (2020).
10. Starr, T. N. *et al.* SARS-CoV-2 RBD antibodies that maximize breadth and resistance to escape. *Nature* **597**, 97–102 (2021).
11. Copin, R. *et al.* The monoclonal antibody combination REGEN-COV protects against SARS-CoV-2 mutational escape in preclinical and human studies. *Cell* **184**, 3949–3961.e11 (2021).
12. Baum, A. *et al.* Antibody cocktail to SARS-CoV-2 spike protein prevents rapid mutational escape seen with individual antibodies. *Science* **369**, 1014–1018 (2020).
13. Liu, Z. *et al.* Identification of SARS-CoV-2 spike mutations that attenuate monoclonal and serum antibody neutralization. *Cell Host & Microbe* **29**, 477–488.e4 (2021).
14. Corti, D., Purcell, L. A., Snell, G. & Veisler, D. Tackling COVID-19 with neutralizing monoclonal antibodies. *Cell* **184**, 3086–3108 (2021).
15. Hershowe, J., Kightlinger, W. & Jewett, M. C. Cell-free systems for accelerating glycoprotein expression and biomanufacturing. *Journal of Industrial Microbiology and Biotechnology* **47**, 977–991 (2020).
16. Silverman, A. D., Karim, A. S. & Jewett, M. C. Cell-free gene expression: an expanded repertoire of applications. *Nature Reviews Genetics* **21**, 151–170 (2020).
17. Ojima-Kato, T., Nagai, S. & Nakano, H. Ecobody technology: rapid monoclonal antibody screening method from single B cells using cell-free protein synthesis for antigen-binding fragment formation. *Scientific Reports* **7**, 13979 (2017).
18. Ojima-Kato, T. *et al.* ‘Zipbody’ leucine zipper-fused Fab in E. coli in vitro and in vivo expression systems. *Protein Engineering Design and Selection* **29**, 149–157 (2016).
19. Ojima-Kato, T. *et al.* Rapid Generation of Monoclonal Antibodies from Single B Cells by Ecobody Technology. *Antibodies* **7**, 38 (2018).

20. Murakami, S., Matsumoto, R. & Kanamori, T. Constructive approach for synthesis of a functional IgG using a reconstituted cell-free protein synthesis system. *Scientific Reports* **9**, 671 (2019).
21. Martin, R. W. *et al.* Development of a CHO-Based Cell-Free Platform for Synthesis of Active Monoclonal Antibodies. *ACS Synthetic Biology* **6**, 1370–1379 (2017).
22. Stech, M. & Kubick, S. Cell-Free Synthesis Meets Antibody Production: A Review. *Antibodies* **4**, 12–33 (2015).
23. Cai, Q. *et al.* A simplified and robust protocol for immunoglobulin expression in *Escherichia coli* cell-free protein synthesis systems. *Biotechnology Progress* **31**, 823–831 (2015).
24. Yasgar, A., Jadhav, A., Simeonov, A. & Coussens, N. P. AlphaScreen-Based Assays: Ultra-High-Throughput Screening for Small-Molecule Inhibitors of Challenging Enzymes and Protein-Protein Interactions. in *Methods in Molecular Biology* vol. 1439 77–98 (2016).
25. Brouwer, P. J. M. *et al.* Potent neutralizing antibodies from COVID-19 patients define multiple targets of vulnerability. *Science* **369**, 643–650 (2020).
26. Barnes, C. O. *et al.* Structures of human antibodies bound to SARS-CoV-2 spike reveal common epitopes and recurrent features of antibodies. *Cell* 2020.05.28.121533 (2020) doi:10.1016/j.cell.2020.06.025.
27. Du, S. *et al.* Structurally Resolved SARS-CoV-2 Antibody Shows High Efficacy in Severely Infected Hamsters and Provides a Potent Cocktail Pairing Strategy. *Cell* 1–11 (2020) doi:10.1016/j.cell.2020.09.035.
28. Piccoli, L. *et al.* Mapping Neutralizing and Immunodominant Sites on the SARS-CoV-2 Spike Receptor-Binding Domain by Structure-Guided High-Resolution Serology. *Cell* **183**, 1024–1042.e21 (2020).
29. Kreye, J. *et al.* A Therapeutic Non-self-reactive SARS-CoV-2 Antibody Protects from Lung Pathology in a COVID-19 Hamster Model. *Cell* **183**, 1058–1069.e19 (2020).
30. Ju, B. *et al.* Human neutralizing antibodies elicited by SARS-CoV-2 infection. *Nature* **584**, 115–119 (2020).
31. Shi, R. *et al.* A human neutralizing antibody targets the receptor-binding site of SARS-CoV-2. *Nature* **584**, 120–124 (2020).
32. Liu, L. *et al.* Potent neutralizing antibodies against multiple epitopes on SARS-CoV-2 spike. *Nature* **584**, 450–456 (2020).
33. Barnes, C. O. *et al.* SARS-CoV-2 neutralizing antibody structures inform therapeutic strategies. *Nature* **588**, 682–687 (2020).
34. Yuan, M. *et al.* A highly conserved cryptic epitope in the receptor binding domains of SARS-CoV-2 and SARS-CoV. *Science* **368**, 630–633 (2020).
35. Wu, Y. *et al.* A noncompeting pair of human neutralizing antibodies block COVID-19 virus binding to its receptor ACE2. *Science* **368**, 1274–1278 (2020).
36. Cao, Y. *et al.* Potent Neutralizing Antibodies against SARS-CoV-2 Identified by High-Throughput Single-Cell Sequencing of Convalescent Patients' B Cells. *Cell* **182**, 73–84.e16 (2020).
37. Chi, X. *et al.* A neutralizing human antibody binds to the N-terminal domain of the Spike protein of SARS-CoV-2. *Science* **369**, 650–655 (2020).

38. Hansen, J. *et al.* Studies in humanized mice and convalescent humans yield a SARS-CoV-2 antibody cocktail. *Science* **369**, 1010–1014 (2020).
39. Yuan, M. *et al.* Structural basis of a shared antibody response to SARS-CoV-2. *Science* **369**, 1119–1123 (2020).
40. Tortorici, M. A. *et al.* Ultrapotent human antibodies protect against SARS-CoV-2 challenge via multiple mechanisms. *Science* **370**, 950–957 (2020).
41. Ding, R. *et al.* Rapid isolation of antigen-specific B-cells using droplet microfluidics. *RSC Advances* **10**, 27006–27013 (2020).
42. Sun, Z. Z., Yeung, E., Hayes, C. A., Noireaux, V. & Murray, R. M. Linear DNA for rapid prototyping of synthetic biological circuits in an escherichia coli based TX-TL cell-free system. *ACS Synthetic Biology* **3**, 387–397 (2014).
43. Ritz, D. *et al.* Conversion of a Peroxiredoxin into a Disulfide Reductase by a Triplet Repeat Expansion. *Science* **294**, 158–160 (2001).
44. Kim, D.-M. & Swartz, J. R. Efficient production of a bioactive, multiple disulfide-bonded protein using modified extracts of Escherichia coli. *Biotechnology and Bioengineering* **85**, 122–129 (2004).
45. Yin, G. & Swartz, J. R. Enhancing Multiple Disulfide Bonded Protein Folding in a Cell-Free System. *Biotechnology and Bioengineering* **86**, 188–195 (2004).
46. Dopp, J. L. & Reuel, N. F. Simple, functional, inexpensive cell extract for in vitro prototyping of proteins with disulfide bonds. *Biochemical Engineering Journal* **164**, 107790 (2020).
47. Groff, D. *et al.* Engineering toward a bacterial “endoplasmic reticulum” for the rapid expression of immunoglobulin proteins. *mAbs* **6**, 671–678 (2014).
48. Ryabova, L. A., Desplancq, D., Spirin, A. S. & Plückthun, A. Functional antibody production using cell-free translation: Effects of protein disulfide isomerase and chaperones. *Nature Biotechnology* **15**, 79–84 (1997).
49. Carter, P. *et al.* Humanization of an anti-p185HER2 antibody for human cancer therapy. *Proceedings of the National Academy of Sciences* **89**, 4285–4289 (1992).
50. Benjamini, Y. & Hochberg, Y. Controlling the False Discovery Rate: A Practical and Powerful Approach to Multiple Testing. *Journal of the Royal Statistical Society: Series B (Methodological)* **57**, 289–300 (1995).
51. Greaney, A. J. *et al.* Comprehensive mapping of mutations in the SARS-CoV-2 receptor-binding domain that affect recognition by polyclonal human plasma antibodies. *Cell Host & Microbe* **29**, 463-476.e6 (2021).
52. Tan, C. W. *et al.* A SARS-CoV-2 surrogate virus neutralization test based on antibody-mediated blockage of ACE2–spike protein–protein interaction. *Nature Biotechnology* **38**, 1073–1078 (2020).
53. Wrobel, A. G. *et al.* Antibody-mediated disruption of the SARS-CoV-2 spike glycoprotein. *Nature Communications* **11**, 5337 (2020).